



Phylogeography and population structure of *Ponticola gorlap* (Teleostei: Gobiidae) in an evolutionary distinctive and ecologically threatened Caspian Sea sub-basin

Fatah Zarei¹ · Hamid Reza Esmaili¹ · Reza Sadeghi² · Bettina Reichenbacher³ · Ulrich K. Schliewen⁴ · Keyvan Abbasi⁵ · Ali Gholamhosseini¹

Received: 9 January 2022 / Accepted: 1 November 2022 / Published online: 17 November 2022

© The Author(s), under exclusive licence to Springer Nature Switzerland AG 2022

Abstract

The South Caspian Sea sub-basin, owing to its complex paleogeographic history and habitat diversity, represents a center of endemism and a high-priority conservation area for the gobiid genus *Ponticola*. However, very little is currently known about most biological aspects of these species in general, and this sub-basin is highly threatened by anthropogenic activities. Here we examined the phylogeographic patterns, genetic diversity, and population structure of the endemic Caspian Sea species *P. gorlap*, in this evolutionary distinctive and ecologically threatened Caspian sub-basin. Mitochondrial DNA control region sequences and otolith shape variations were analyzed from 472 individuals at seven South Caspian localities. Results showed: (i) two shared and eight private haplotypes, distinguished by shallow divergences, (ii) pairwise Φ_{ST} values among locations, ranging from -0.052 to 1.00 ; with most of the highest between Sefidroud/Kaboudval and the other samples, (iii) genetic diversity was generally low, smaller at Kaboudval/Nekaroud, and highest at Babolroud, (iv) non-unimodal mismatch distribution and neutrality tests both rejected a recent demographic expansion scenario, (v) otolith shape analysis revealed significant differences among samples, the highest between Sefidroud/Kaboudval and the others, and (vi) Mantel tests confirmed that both pairwise Φ_{ST} and otolith shape differences were more correlated to each other than with geographic distances. Different scenarios are discussed to explain the observed patterns of genetic and otolith shape variations and population structure of *P. gorlap*, including possible roles of euryhalinity, and presence of migratory and resident forms.

Keywords Caspian bighead goby · Genetic diversity · Mitochondrial DNA · Otolith shape

Introduction

The Caspian Sea basin has a complex paleogeographic history (e.g., Krijgsman et al. 2019) and according to Naseka and Bogutskaya (2009), it harbors more than 159 extant species and subspecies of indigenous fishes, of which > 60% are endemic. Most prominent in terms of endemic biodiversity are the members of the teleost family Gobiidae *sensu* Gill and Mooi 2012 (Naseka and Bogutskaya 2009). Indigenous gobi fauna of this basin, which vary considerably with latitude, presently include 41 species in 11 genera (Zarei et al. 2022a). North, Middle, and South Caspian Sea sub-basins each harbor 20, 30, and 37 gobiid species, and 0, 3 and 10 species sub-basin endemics, respectively. The present high diversity and endemism of Gobiidae in the South Caspian Sea sub-basin could be caused by: (i) high ecological diversity (e.g., sea water depth range, freshwater abundance, and habitat variability) that has led to differential

✉ Hamid Reza Esmaili
hresmaeili@shirazu.ac.ir

¹ Ichthyology and Molecular Systematics Research Laboratory, Zoology Section, Department of Biology, School of Science, Shiraz University, Shiraz, Iran

² Department of Biology, Borujerd Branch, Islamic Azad University, Borujerd, Iran

³ Department of Earth and Environmental Sciences, Palaeontology and Geobiology, Ludwig-Maximilians-Universität, Munich, Germany

⁴ Department of Ichthyology, SNSB-Bavarian State Collection of Zoology, Münchhausenstr. 21, 81247 Munich, Germany

⁵ Inland Waters Aquaculture Research Center, Iranian Fisheries Sciences Research Institute, Bandar Anzali, Iran

niche adaptation and adaptive radiation in several genera (Boldyrev and Bogutskaya 2007; Zarei et al. 2021), (ii) presently less limiting conditions in the South compared with the North Caspian Sea, i.e., higher present-day winter minimum water temperatures and higher water salinity (Naseka and Bogutskaya 2009), (iii) higher extinction rates at Caspian higher latitudes, which were more exposed to the extremes of the Pleistocene climatic and hydrologic changes (Zarei et al. 2022b, c), and (iv) during the Pleistocene climatic oscillations, freshwater habitats of the South Caspian Sea sub-basin may have acted as an evolutionary speciation stage for the gobiid genus *Ponticola* Iljin 1927, since all presently known freshwater endemic species of this genus in the basin are constrained to the South Caspian Sea sub-basin (Eagderi et al. 2020; Vasil'eva et al. 2015; Zarei et al. 2021). This high gobiid diversity and conservation concerns for the South Caspian Sea sub-basin are contrasted by the facts that there is very little known about most biological aspects of these species (Miller 2003, 2004), and this region is being highly ecologically impacted by anthropogenic activities (Esmaeili et al. 2015; Mousavi-Sabet 2021).

Ponticola, an endemic gobiid genus to the Black and Caspian Sea basins, is a monophyletic lineage within the radiation of Paratethyan gobies (Neilson and Stepien 2009). This ecologically diverse group includes several exclusively freshwater species, most endemic to small areas within the Caucasus biodiversity hotspot (Zarei et al. 2022b); and several species restricted to brackish water. In addition, *P. kessleri* (Günther 1861) and *P. gorlap* (Iljin in Berg 1949) are euryhaline species. *Ponticola gorlap*, endemic to the Caspian Sea basin, is a demersal fish found in brackish inshore habitats (usually at 0.5–10 m and rarely at 10–20 m depth) and a wide range of freshwater environments, whose wide tolerance and distribution makes it ecologically unique among presently-known Caspian gobiid species (Zarei et al. 2021). It was first identified in the Caspian Sea as *Gobius kessleri* Günther by Kessler (1874), who found some morphological differences between the Caspian and Black Sea forms. Based on several morphological differences, Iljin (1956) suggested that the Caspian gobies from the Mangyshlak region (western Kazakhstan) merited separation as a distinct species, which he described as *G. gorlap*. Later, karyological, cranial, head scale and morphometric data in samples from the Dnieper, Dniester and Volga rivers supported specific status of the Mangyshlak samples (Vasil'ev and Vasil'eva 1992), and subsequently, it was described as a separate species by Vasil'eva and Vasil'ev (1996), who regarded the species name *gorlap* as invalid and proposed the new name *iljini*, which later was synonymized with *Ponticola gorlap* (Iljin) in a modern phylogenetic systematic study (Neilson and Stepien 2009). Vasil'eva et al. (2016) reestablished the validity of *P. iljini* based on karyological data, but restricted its distribution to the coast of the Mangyshlak Peninsula in western Kazakhstan. *Ponticola kessleri*, *P. iljini*, and *P. gorlap*

form independent phyletic lineages within a clade of *Ponticola* (Neilson and Stepien 2009; Vasil'eva et al. 2016). Further studies on the phylogeography and population structure of these species, may provide valuable insights into their past evolutionary history and diversification.

Surveys of genetic diversity, phylogeographic patterns and population structure of species are crucial to understand the degree of gene flow and connectivity among populations, and to identify isolated populations/lineages and their respective evolutionary histories (e.g., Esmaeili et al. 2020; Mehraban et al. 2020). The amount and geographic patterns of genetic diversity affect the adaptability of populations to changing environments, and thus impact their long-term survival (e.g., Ouborg et al. 2010), thus providing important information for designing effective habitat management and conservation plans. Phylogeographic pattern and population structure of the euryhaline fish, *P. gorlap* in the Caspian Sea basin appear complex and may be influenced by several factors: (i) the species' ability to inhabit both saline and freshwater habitats; (ii) possible presence of migratory and sedentary (riverine) forms; (iii) fluctuating sea water levels associated with Pliocene and Pleistocene glaciations (Reid and Orlova 2002; Zarei et al. 2021, 2022b, c); (iv) genetic isolation by geographic distance (IBD, Slatkin 1993) across its wide distributional range; and (v) anthropogenic modification of natural systems in the basin. Herein, we assessed the genetic diversity, phylogeography and population structure of *P. gorlap* in the South Caspian Sea sub-basin (SCB), using variable sequences of the mitochondrial DNA (mtDNA) control region (CR) in comparison to sagittal otolith shape analysis using wavelet transformation in shapeR (Libungan and Pálsson 2015). Otolith analysis has made significant contributions to the understanding of systematics and evolution of various teleost fishes (e.g., Reichenbacher et al. 2007), with otolith shapes being influenced by a mixture of genetic variability and regional environmental variables (e.g., Berg et al. 2018; Cardinale et al. 2004). Otolith shape analysis provides a morphological tool for studying intraspecific patterns of diversity and a phenotypic basis for evaluating variation among fish stocks and population variants within and among fishery management units (e.g., Libungan et al. 2015; Sadeghi et al. 2020; Reichenbacher et al. 2009). Results may shed light on diversity and distribution of this species in the SCB, necessary for formulating conservation strategies and management proposals.

Materials and methods

Study sites, sampling and preservation

Samples of *Ponticola gorlap* (472 specimens) were investigated from seven localities, each situated in a hydrographic

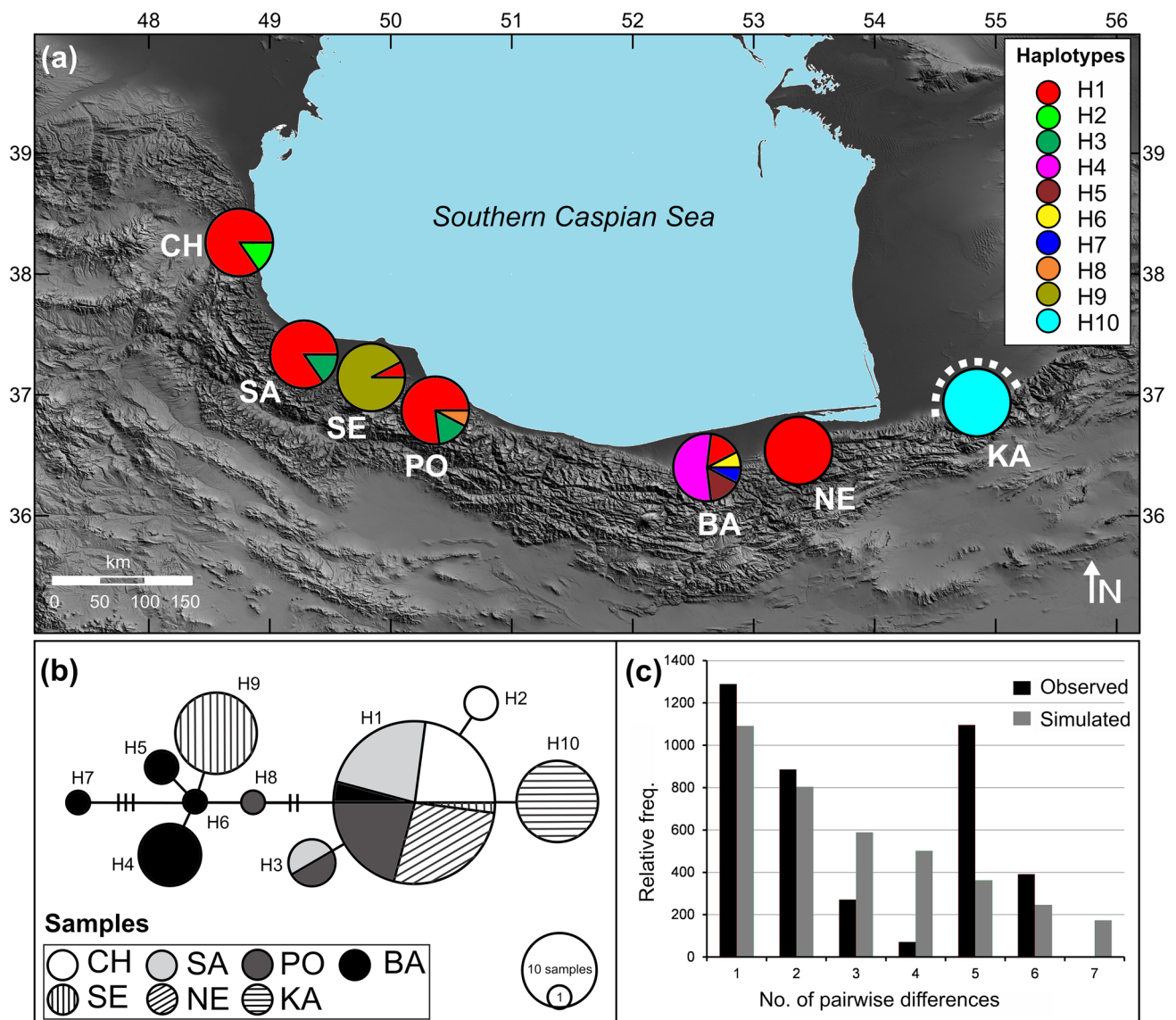


Fig. 1 **a** Sampling sites for *Ponticola gorlap* and distributions of their observed mitochondrial haplotypes (control region; 10 haplotypes, 90 individuals; each color indicates a haplotype) in the South Caspian Sea sub-basin (SCB). Samples: Chalvand (CH), Siahdarvishan (SA), Sefidroud (SE), Polroud (PO), Babolroud (BA), Nekaroud (NE), and Kaboudval (KA). The dotted white line refers to the isolation of the KA sample above the Zarrin Gol Dam (=Kaboudval Dam). **b** The MJ haplotype network for 10 mitochondrial haplotypes observed in seven *P. gorlap* samples in the SCB. The circle area is proportional

to the frequency of each haplotype. Each color/fill pattern indicates a sampling site; each soft line connecting neighboring haplotypes represents a single mutational step, and the lines with small black hatch marks indicate multiple mutational steps between sampled haplotypes. **c** MMD for the pooled DNA sequences of *P. gorlap* in the SCB. The observed distribution (black bars) are compared for their goodness-of-fit with a Poisson distribution under a model of sudden expansion illustrated by the gray bars

area of the SCB: the Chalvand (CH), Siahdarvishan (SA), Sefidroud (SE), Polroud (PO), Babolroud (BA), and Nekaroud (NE) rivers and Kaboudval (KA) stream (Fig. 1a; Table 1). Specimens were collected with electro-fishing between August and October 2019, using quinaldine sulphate as an anesthetic. The right pectoral fin of each specimen was fixed in 96% ethanol for molecular analysis, while the voucher specimens were kept in 70% ethanol for otolith

extraction and shape analysis. These specimens are deposited in the Zoological Museum of Shiraz University, Collection of Biology Department (ZM-CBSU; Table 1). To reduce the possible effects of ontogenetic variations on otolith shape, only sexually mature specimens were selected. Standard length (SL) was measured to nearest 0.01 mm with a digital caliper from the most-anterior end of the upper lip to the beginning of the caudal fin rays.

Table 1 Sampling sites of *Ponticola gorlap* in the SCB, and number of specimens evaluated at each

Code	Population	Coordinates	D-loop		Otolith shape		
			<i>N</i>	GenBank	<i>N</i>	ZM-CBSU	SL range (mean)
CH	Chalvand	38.29, 48.88	13	ON724062–ON724074	71	11/01–71	53.80–99.11 (70.65)
SA	Siahdarvishan	37.35, 49.42	13	ON724075–ON724087	48	13/01–48	41.70–80.69 (58.96)
SE	Sefidroud	37.25, 49.82	13	ON724127–ON724139	55	16/01–55	52.01–95.75 (74.80)
PO	Polroud	37.09, 50.38	13	ON724101–ON724113	40	15/01–40	50.68–102.6 (71.17)
BA	Babolroud	36.51, 52.68	13	ON724088–ON724100	52	10/01–52	51.76–97.74 (72.54)
NE	Nekaroud	36.63, 53.34	13	ON724114–ON724126	70	14/01–70	53.30–84.55 (63.39)
KA	Kaboudval	36.89, 54.89	12	ON724140–ON724151	46	12/01–46	49.24–78.44 (64.55)

N number of specimens, *SL* standard length

DNA extraction and PCR amplification

Genomic DNA was extracted from fin samples preserved in 96% ethanol based on a salt-extraction method, following Bruford et al. (1992). PCR amplification of the mitochondrial control region (D-loop, 423 bp) was performed with the primer pair L-Pro1 and H-DL1 (Ostellari et al. 1996). The 25 µl PCR reaction mixes included 12.5 µl of a 2X Taq PCR Master Mix (Parstous™), 0.5 µl of each primer (10 pmol/µl), 6 µl of the target DNA, and 5.5 µl DNase-free ddH₂O. The PCR conditions were initial denaturation for 3 min at 94 °C followed by 35 cycles of 94 °C for 45 s, 61 °C for 45 s, and 72 °C for 1 min, and final extension for 7 min at 72 °C. PCR products were purified using ExoSAP-IT™ and sequenced by the Niagene Lab (Tehran, Iran) using an Applied Biosystems™ BigDye™ Terminator v3.1 Cycle Sequencing Kit and an Applied Biosystems™ ABI PRISM 3730xl sequencer.

Population genetics and phylogeographic analyses

Control region sequences (423 bp) were edited with BioEdit 7.0.4 (Hall 1999), and aligned with the ClustalW algorithm as implemented in Mega 7.0 (Kumar et al. 2016). All newly obtained sequences are deposited in GenBank (Table 1). The number of polymorphic sites (*s*), number of haplotypes (*H*), haplotype diversity (*H_d*), nucleotide diversity (π), and average number of pairwise nucleotide differences (*k*) were computed with Arlequin 3.5.2.2 (Excoffier and Lischer 2010). Historical demographic patterns were investigated using (a) neutrality tests, including Tajima's *D* and Fu's *F_s* with Arlequin (10,000 permutations) and Ramos-Onsins and Rozas's *R₂* with DnaSP 6 (Librado and Rozas 2009); and (b) mismatch distributions of pairwise differences (MMD) in Arlequin. Designed to evaluate possible deviation from the expectations of the neutral theory (Kimura 1983), the applied neutrality tests differ in their approaches: Tajima's *D* and *R₂* use mutation frequency, whereas Fu's *F_s* uses the haplotype distribution. Arlequin was employed to estimate pairwise Φ_{ST} values among samples. A Bonferroni

correction (0.05/number of tests) was used to correct for multiple tests. Geographic Distance Matrix Generator 1.2.3 (<https://biodiversityinformatics.amnh.org/>) was employed to estimate a geographic distance matrix. Mantel tests were used to evaluate the possible effect of isolation by distance (IBD; Slatkin 1993) with vegan 2.0 (Dixon 2003) in R 4.0.5 (Ihaka and Gentleman 1996). Significance was evaluated at *p* = 0.05, after Bonferroni correction (0.05/number of tests). Divergence and phylogenetic relationships between haplotypes were reconstructed with the median-joining (MJ) method as implemented in PopART 1.7 (Leigh and Bryant 2015).

Otolith imaging and shape analysis

The head region of specimens was dissected under a Zeiss™ Stemi SV6 stereomicroscope. The left sagittae (= left saccular otolith) was extracted with fine tweezers, cleaned by incubation in 1% KOH solution (3 min), washed in distilled water, and then dried at room temperature. To describe the general morphology of *P. gorlap*'s sagittae from the SCB, five otoliths (ZM-CBSU 41, 44–46, and 48; 88.6–110.9 mm SL) from the CH site were coated with gold, and scanning electron microscope (SEM) images were taken using a TESCAN™ VEGA3. Morphological terminology for the sagittae followed Gierl et al. (2018), Schwarzahns et al. (2020), and Reichenbacher and Bannikov (2021), as shown in Fig. 2. Otolith measurements were taken in ImageJ 1.52a.

Left sagittal otoliths of 382 *P. gorlap* specimens from seven south Caspian localities (Table 1) were placed on a dark plate and digital images at 4x magnification were taken with a 14MP Industrial Microscope Camera 180x equipped with an S-EYE 1.2.4.128 image processing system. To measure otolith shape variation, we employed statistical functions in R 4.0.5 (Ihaka and Gentleman 1996) with the packages shapeR 0.1-5 (Libungan and Pálsson 2015), vegan 2.5-7 (Oksanen et al. 2020), ipred 0.9–12 (Peters et al. 2021), and MASS 7.3–54 (Ripley et al. 2021). The otolith images were read into R. ShapeR analyzes otolith shape by extracting otolith outlines from these images. A

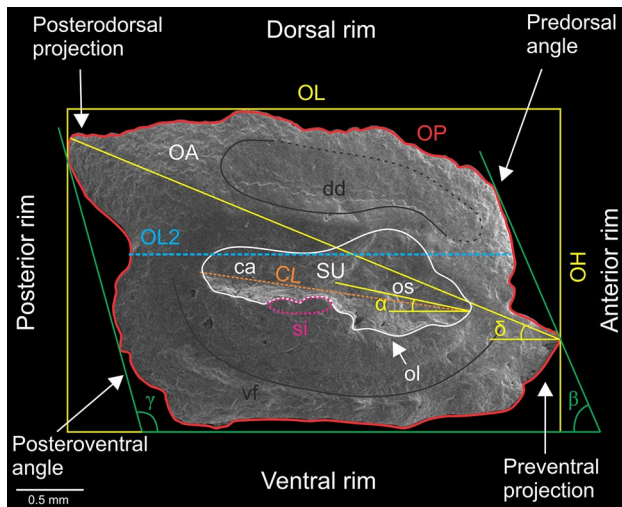


Fig. 2 SEM photo of the *Ponticola gorlap*'s left sagittal otolith (inner face, ZM-CBSU 44, 72.8 mm SL, Chalvand River), showing the terminology of characters and otolith shape outline (red line). *OL* maximal otolith length, *OL2* minimal otolith length measured at maximum ingression of concavity of posterior rim, *OH* maximal otolith height, *OA* otolith area, *OP* otolith perimeter, *SU* sulcus, *ca* cauda, *os* ostium, *ol* ostila lobe, *CL* colliculum length, measured along its axis, *dd* dorsal depression, *vf* ventral furrow, *si* subcaudal igum, α inclination angle of ostium measured from tip of ostium through midpoint of sulcus height at collum, β inclination angle of anterior rim, γ inclination angle of posterior rim; δ , inclination of line connecting preventral projection with tip of posterodorsal projection. Scale bar = 0.5 mm

matrix of coordinates (x , y) from all otolith outlines was calculated. Evenly spaced radii, with length as a univariate shape descriptor, were drawn from the otolith centroid to its outline. Based on the wavelet transformation on radii, the wavelet coefficients were extracted with wavethresh 4.6.8 (Nason 2016). To remove the influence of allometric growth, wavelet coefficients that showed significant ($P < 0.05$) interaction between samples and SL were excluded (Libungan et al. 2015), and the remaining coefficients were imported into the R statistical package. Mean otolith shapes for *P. gorlap* samples were plotted based on the wavelet coefficients. To determine areas of otolith shape variation, mean shape coefficients and their standard deviations were plotted against the angle of the otolith outlines using wavelet transform with gplots 3.1.1 (Warnes et al. 2020). Because the proportion of variation among groups (intraclass correlation) was more informative to measure between-population differences, intraclass correlation was estimated along the otolith outline.

The radii length was employed to test the significance of differences between samples based on an ANOVA-like permutation test (1000 permutations) in vegan. Significance was evaluated at $P = 0.05$, after Bonferroni correction (0.05/number of tests). To investigate the statistical significance of otolith shape difference between males and

females, sexual stability in otolith shape was analyzed in shapeR. The standardized wavelet coefficients were transformed into principal coordinates and subjected to canonical analysis (CAP: Canonical Analysis of Principal coordinates) to assess the variation in otolith shape among the samples. Results were compared among samples based on the function *capscale* in vegan. The wavelet coefficients were further employed for cluster visualization of the CAP results using two discriminating axes (CAP1, CAP2). The CAP outcome was employed as the input for a dendrogram based on the Squared Euclidean Dissimilarity Distance in PAST 3.03 (Hammer et al. 2001). Based on a leave-one-out cross-validation scheme, the classification success into groups was investigated. Accordingly, employing the functions *errorest* and *lda* in ipred and MASS, Linear Discriminant Analysis (LDA) on the standardized wavelet coefficients was conducted to evaluate the classification of individuals to the original samples with cross-validation estimation. A matrix of average Euclidean distances among samples based on otolith shape (CAP1, CAP2) was estimated. Applying the Mantel test (Pearson test, 1000 permutations) as implemented in vegan with R, we tested the hypothesis of regional otolith shape differentiation under IBD. Significance was evaluated at $P = 0.05$, after a Bonferroni correction (0.05/number of tests).

Results

Genetic diversity and phylogeographic pattern

Sequence analysis of a 423 bp fragment of the mtDNA control region detected 10 variable nucleotide sites (2 singleton variable and 8 parsimony informative sites) among 90 *P. gorlap* specimens from seven south Caspian samples, which had a total of 10 haplotypes (H1–H10). Overall haplotype diversity (H_d) was 0.678, ranging from 0.000 for NE and KA (one haplotype per site) to 0.705 (4 haplotypes) for BA (Table 2). Overall nucleotide diversity (π) was 0.00471, ranging from 0.000 for NE and KA to 0.00491 for BA. The higher and lower levels of H_d and π in NE and KA, and BA were also evident in the higher and lower values of their average number of pairwise nucleotide differences (k ; 0.000, 0.000, and 2.077, respectively).

Of 10 mitochondrial haplotypes, eight (80%) were site specific, H2 to CH, H4–H7 to BA, H8 to PO, H9 to SE, and H10 to KA, whereas H1 and H3 were shared among samples (Table 3; Fig. 1a). H1, the most common haplotype (48 specimens) with the highest frequencies in NE, CH, SA and PO was found in all the studied samples except for KA, while H3 was shared between SA and PO (2 specimens each). In the reconstructed MJ haplotype network (Fig. 1b),

Table 2 Genetic diversity (control region) and neutrality test results for the samples of *Ponticola gorlap*

	N	H	s	Hd±SD	π±SD	k±SD	Tajima's D	Fu's Fs	R2
CH	13	2	1	0.282±0.14	0.00067±0.00086	0.282±0.32	0.274	0.240	0.141
SA	13	2	1	0.282±0.14	0.00067±0.00086	0.282±0.32	-0.274	0.240	0.141
BA	13	5	7	0.705±0.12	0.00491±0.00330	2.077±1.24	-0.301	0.028	0.148
PO	13	3	3	0.410±0.15	0.00139±0.00134	0.590±0.50	-1.233	-0.248	0.184
NE	13	1	0	0.000±0.00	0.00000±0.00000	0.000±0.00	0.000	0.000	NA
SE	13	2	4	0.154±0.13	0.00146±0.00138	0.615±0.52	-1.775*	1.47	0.266
KA	12	1	0	0.000±0.00	0.00000±0.00000	0.000±0.00	0.000	0.000	NA
Total	90	10	10	0.678±0.05	0.00471±0.00297	1.994±1.14	0.0289	-0.963	0.0997

H number of haplotypes, *Hd* haplotype diversity, *k* average number of nucleotide differences, *N* sample size, *s* number of polymorphic sites, *SD* standard deviation, *π* nucleotide diversity, *NA* not applicable
* *P* < 0.05

Table 3 Haplotype frequencies (relative frequency) of 10 mitochondrial haplotypes in the samples

	N	H1	H2	H3	H4	H5	H6	H7	H8	H9	H10
CH	13	11 (0.85)	2 (0.15)	0	0	0	0	0	0	0	0
SA	13	11 (0.85)	0	2 (0.15)	0	0	0	0	0	0	0
BA	13	2 (0.15)	0	0	7 (0.54)	2 (0.15)	1 (0.08)	1 (0.08)	0	0	0
PO	13	10 (0.77)	0	2 (0.15)	0	0	0	0	1 (0.08)	0	0
NE	13	13 (1.00)	0	0	0	0	0	0	0	0	0
SE	13	1 (0.08)	0	0	0	0	0	0	0	12 (0.92)	0
KA	12	0	0	0	0	0	0	0	0	0	12 (1.00)

N sample size

Table 4 Pairwise Φ_{ST} values between the samples (below the diagonal)

	CH	SA	SE	PO	BA	NE	KA
CH		0.235	<1E-6	0.234	<1E-6	0.498	<1E-6
SA	0.083		<1E-6	0.999	<1E-6	0.462	<1E-6
SE	0.883	0.883		<1E-6	<1E-6	<1E-6	<1E-6
PO	0.056	-0.052	0.838		<1E-6	0.476	<1E-6
BA	0.655	0.659	0.452	0.604		<1E-6	<1E-6
NE	0.083	0.083	0.917	0.042	0.686		<1E-6
KA	0.873	0.873	0.932	0.767	0.751	1.000	

The upper triangular matrix shows P-values from the pairwise comparisons. The Bonferroni correction for comparisons among all samples was 0.05/21 = 0.00238. Values in bold type are significant after correction for multiple tests

all haplotypes were closely related, deviating by mostly one, or rarely two (H6/H7) or three (H1/H8) nucleotides.

Genetic differences among samples

Pairwise Φ_{ST} values between *P. gorlap* sampling sites were low to high, ranging from -0.052 between SA/PO to 1.00 between NE/KA (Table 4). CH, SA and PO showed the highest Φ_{ST} values for those being geographically close (i.e., SE: 0.883, 0.883, and 0.838, respectively; *P* < 0.001) and distant samples (i.e., KA: 0.873, 0.873, and 0.767, respectively;

P < 0.001). The Φ_{ST} values between BA and other samples [except for SE (0.452, *P* < 0.001)] were moderately high and statistically significant (*P* < 0.001), ranging from 0.604 for PO to 0.751 for KA. NE had the lowest Φ_{ST} value with PO (0.042, *P* > 0.05), and the highest genetic distances with SE (0.917) and KA (1.000). Accordingly, SE and KA often showed high and statistically significant Φ_{ST} values from other *P. gorlap* samples. Furthermore, even with a Bonferroni correction for multiple tests (21 pairwise tests, *P* < 0.05/21 = 0.00238 for significance at the 5% level), there are significant differentiations between the above-mentioned

samples (Table 4). IBD analysis using the Mantel test showed a moderate but statistically significant positive correlation between the pairwise Φ_{ST} and geographic distance matrices ($r=0.473$, $P=0.008$).

Historical changes in effective population size

Tajima's D values for CH, SA, BA, PO, and SE were negative, suggesting an excess of rare substitutions under the expectation of a neutral model of evolution; however, these departures from neutrality were not significant ($P>0.05$) except for SE. Fu's F_s values were non-significantly ($P>0.02$) positive for CH, SA, BA and SE, and negative for PO ($P>0.02$). Similarly, Ramos-Onsins and Rozas's R_2 values were non-significantly low ($P>0.05$) [not applicable for NE and KA]. *Ponticola gorlap*, as a whole, showed non-significant positive D ($P>0.05$), negative F_s ($P>0.02$), and low R_2 ($P>0.05$) values. The observed MMD (Fig. 1c) for the pooled data set was not unimodal and thus did not support a model of sudden expansion (Harpending 1994). Therefore, non-significant neutrality tests and non-unimodal MMD reject a recent expansion model for areas and for *P. gorlap* as a whole in the SCB.

General morphology of *P. gorlap*'s otolith

The otoliths of *P. gorlap* from the SCB have a parallelogram shape, with marked pre-ventral and postero-dorsal projections (Fig. 2). The otolith length to height (OL/OH) ratio is 1.32–1.58; the dorsal rim slightly ascends posteriorly, somewhat irregularly undulating or coarsely; the pre-dorsal angle is obtuse; the postero-dorsal projection is long, pointed or blunt, and slightly or strongly bent outwards. The anterior rim usually lacks incision, or is sometimes slightly incised at to slightly above the level of ostium, inclined at 66.12–81.25° (β). The posterior rim is almost parallel to the anterior rim or a little less oblique, and is inclined at 92.5–104.6° (γ), with a marked concavity (incision or notch) below the postero-dorsal projection at or slightly above the level of the cauda. The angle of the pre-ventral to post-dorsal traverse is 24–28° (δ). The ventral rim is horizontal, smooth or slightly undulating, slightly projecting downwards near the posterior end; the pre-ventral projection is long, pointed or blunt; the postero-ventral angle is usually broadly rounded, or sometimes undulated. The sulcus is centrally positioned, sole-shaped, anteriorly inclined at 9.4–18.81° (α), deep with a well-developed ostial lobe. The sulcus is long (OL2/CL: 1.40–1.51), and relatively wide. The subcaudal iugum is present, short (1/3 cauda length), slender, and located below the anterior part of the cauda. The ventral furrow runs with a moderate or close distance to the ventral rim, curving upwards anteriorly to the level of the ostial apex and turning upwards to the level of the caudal tip or slightly behind

it. The dorsal depression ranges from distinct to indistinct, and is narrow to moderately wide. The inner surface of the otolith is convex, while the outer face is concave.

Univariate otolith shape analysis based on radii

In total, otoliths of 382 *Ponticola gorlap* individuals (from seven samples) were analyzed. Results of the ANOVA-like permutation test using the radii found no significant differences between male and female otolith shapes (F -value = 1.2647, $P=0.247$) and the CAP analysis based on PC1 of the wavelet coefficients detected no significant differences ($P>0.05$). Thus, male and female otolith samples from each sampling site were combined together in subsequent analyses. According to the results of the ANOVA-like permutation tests and applying a Bonferroni correction for multiple tests (21 pairwise tests, $P<0.05/21=0.00238$ for significance at the 5% level), the lengths of the three major radii statistically differed among all samples ($P<0.01$, Table 5), with the difference between KA and SE being the highest (F -value = 82.28; $P=0.001$).

Differences in mean otolith shape

The mean shape of the otoliths based on the wavelet coefficients differed among the population samples at the pre-ventral projection, anterior rim, anterior half of the dorsal rim, postero-dorsal projection, posterior rim, postero-ventral angle, and the posterior third of ventral rim (Fig. 3a). At the pre-ventral projection (355–20°), SE presents the outermost mean otolith outline (the longest pre-ventral projection) followed by PO, moving toward the otolith centroid in the innermost part is KA (shortest pre-ventral projection). Similarly, at the anterior rim (20–45°), SE and KA have the outermost and innermost mean otolith outlines, respectively. At the pre-dorsal angle (50–85°), this pattern is reversed. According to the mean otolith shape at the anterior rim and pre-dorsal angle, KA and SE have the most right and most obtuse pre-dorsal angles, respectively. From the pre-dorsal angle running posteriorwards to the middle of the dorsal rim (85–135°), SE presents the innermost outline. At the postero-dorsal projection (160–180°), SE in the outermost part has a shape that slightly bends outwards and farthest from the centroid (longest postero-dorsal projection), and moving inward, CH is in the innermost part (the shortest postero-dorsal projection). Below the postero-dorsal projection and above the level of the posterior incision (180–200°), KA and CH have the outermost and innermost outlines, respectively. At the level of the posterior incision, NE presents the innermost outline. Below the incision at the postero-ventral angle (205–240°), NE and KA, and SE and CH show the innermost and outermost mean otolith outlines, respectively. Below the angle running towards the ventral rim (245–305°),

Table 5 ANOVA-like permutation test of the otolith shape between samples (1000 permutations)

Comparison	df ^a	SS ^b	F-value	P ^c
BA v. CH	1	17.96	24.31	0.001
BA v. KA	1	32.38	48.76	0.001
BA v. NE	1	16.99	36.78	0.001
BA v. PO	1	4.34	5.78	0.001
BA v. SA	1	8.17	12.98	0.001
BA v. SE	1	14.62	19.87	0.001
CH v. KA	1	28.78	47.32	0.001
CH v. NE	1	16.99	33.19	0.001
CH v. PO	1	3.17	11.54	0.001
CH v. SA	1	9.27	18.23	0.001
CH v. SE	1	37.96	60.51	0.001
KA v. NE	1	13.57	30.71	0.001
KA v. PO	1	16.88	27.74	0.001
KA v. SA	1	12.97	30.2	0.001
KA v. SE	1	47.85	82.28	0.001
NE v. PO	1	2.37	6.34	0.001
NE v. SA	1	4.54	13.91	0.001
NE v. SE	1	17.19	42.48	0.001
PO v. SA	1	6.68	10.36	0.001
PO v. SE	1	4.09	6.58	0.002
SA v. SE	1	21.5	44.55	0.001

The Bonferroni correction for comparisons among all samples was $0.05/21 = 0.00238$. Values in bold type are significant after correction for multiple tests

^a Degree of freedom

^b Sum of squares

^c P value

NE and KA in the mean shape are in the outermost part, and with moving inwards the otolith centroid, SE and BA similarly show the innermost mean otolith outlines.

These results are further confirmed by the boxplots of the canonical score distances with respect to variation among the samples of *P. gorlap* based on the wavelet coefficients (Fig. 3b). The canonical distances indicate shape differences between KA and the other samples, but no significant differences occurred among all of the other samples. A hierarchical cluster analysis dendrogram based on CAP1 and CAP2 and with Euclidean distance used as a measure of dissimilarity had two main clusters, with KA in one, and the remaining samples in the other (Fig. 3c). The first two discriminate axes of the CAP analysis based on the wavelet coefficients explained 76.5% (CAP1 = 43.6%, CAP2 = 32.9%) of the variation among samples, with clear differences between KA, SE, and the others (Fig. 3d). The overall classification success with a leave-one-out cross-validation estimation was 30.9%; the highest classification value was achieved for KA (71.7%), followed by SE (58.2%) (Table 6). The Mantel test based on 1000 permutations described a moderate positive

correlation between otolith shape variation (Table 7) and the geographical distances among samples ($r = 0.52$, $P = 0.005$). Otolith shape resemblance between samples reflected their genetic distances ($r = 0.77$, $P < 0.001$).

Discussion

Phylogeographic assessments using matrilineal markers provide critical data about evolutionary history, diversity, population structure and connectivity among populations (Stepien and Kocher 1997). Sequence analysis of *P. gorlap* specimens from the SCB revealed a shallow genealogy with variable haplotype distributions (i.e., allopatric and sympatric; see pattern explanation by Avise et al. 1987), indicating recent gene flow among our samples throughout the South Caspian Sea sub-basin. Here, H1 may be the plesiomorphic condition of *P. gorlap* in the SCB, because: (i) it was the most common haplotype, occurring in 48 (53.3%) of 90 assayed individuals; (ii) it was spatially widespread, found in six of the seven investigated sampling sites; and (iii) in the haplotype network, this haplotype connected separately with four other haplotypes in the SCB. Except for H3, each of the eight private haplotypes (H2, H4–H10) was confined to a single locality.

The recurrent and dramatic lake-level fluctuations and salinity changes of the Caspian Sea during the Pliocene and over the Pleistocene glacial cycles (e.g., Forte et al. 2013; Krijgsman et al. 2019) are hypothesized to have had a significant effect on the diversity of its aquatic biota (e.g., Brown and Stepien 2008; Sands et al. 2019; Zarei et al. 2021, 2022a, b, c), including the formation of periodic temporal refugia in South Caspian Sea sub-basin or in riverine systems in the course of low sea level periods or through periods of increased salinity. Loss of connectivity among these refugia may have produced phylogeographic breaks within species (Gante et al. 2009). Considering the pattern observed here, the hypothesis that major low sea level periods in the Caspian Sea and salinity shifts during the Quaternary influenced phylogeographic structure in *P. gorlap* in the SCB is not supported. There was no trace of bottleneck in effective population size, which may be due to the species broad distribution, salinity and temperature tolerance, and ongoing gene flow. Dispersal opportunities likely were abundant during high sea levels, which may have promoted the homogenization of *P. gorlap* haplotypes across the SCB and/or their current distributions and patterns may be a recent phenomenon.

A phylogeographic pattern may reflect IBD, which implies that distance-dependent connectivity limits genetic differences among samples (Slatkin 1993), whose traces have been described in numerous fish species (e.g., Crookes and Shaw 2016; O'Dwyer et al. 2021). Since the *P. gorlap*

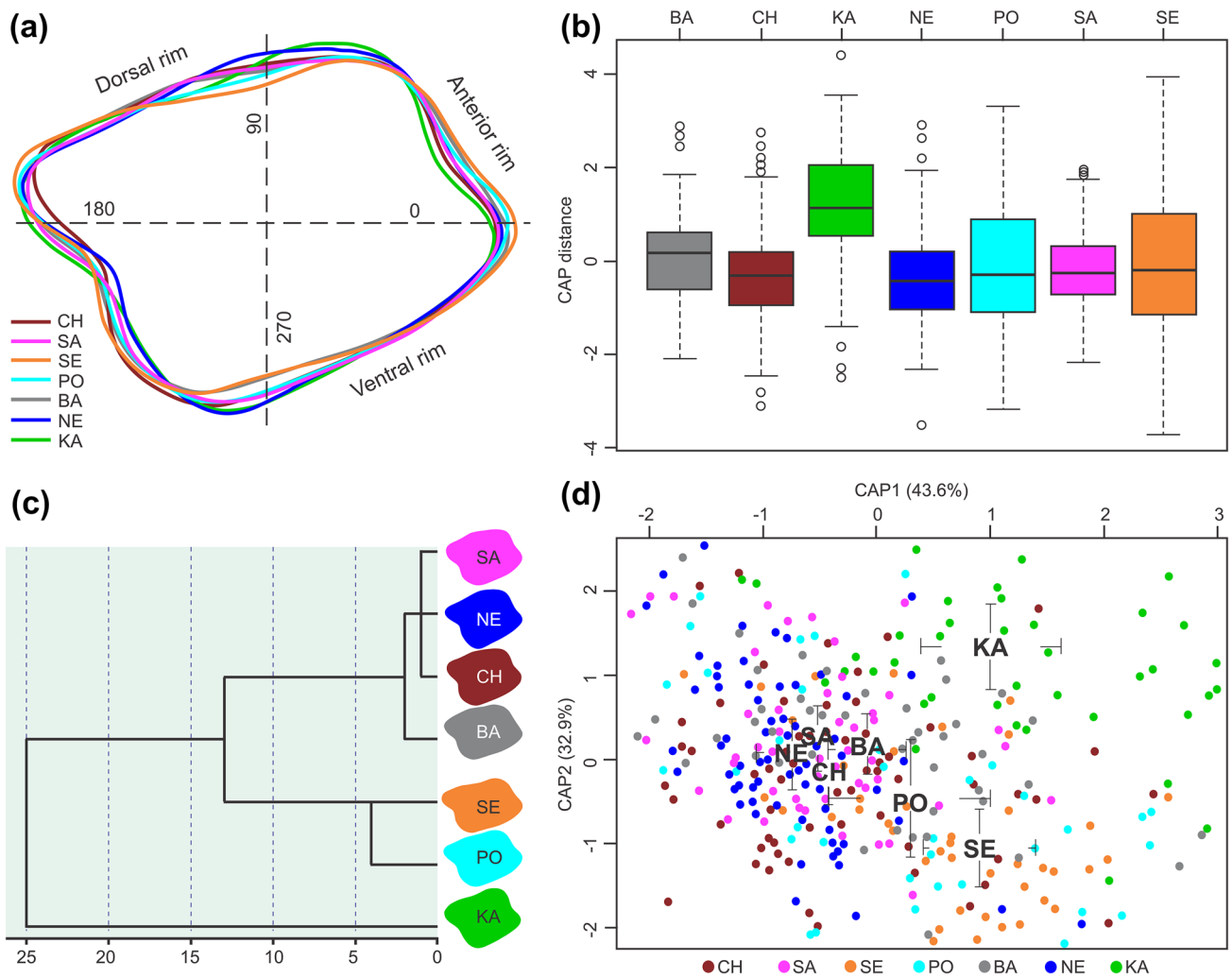


Fig. 3 **a** Mean otolith shapes based on wavelet reconstruction for the *Ponticola gorlap* samples. The numbers 0, 90, 180 and 270 indicate angle in degrees (°) on the outline. **b** Boxplots of canonical score distances with respect to variation among *P. gorlap* samples based on the wavelet coefficients. **c** Hierarchical Cluster Analysis based on otolith shape data (CAP1, CAP2) and using the Euclidean distance

showing the phenotypic relations among samples (mean otolith shapes are depicted on the right). **d** Canonical scores on discriminating axes 1 (CAP1) and 2 (CAP2) for each *P. gorlap* sample using wavelet methodology. Individual data points are indicated by the colored circles

Table 6 Classification values based on Linear Discriminant Analysis of the standardized wavelet coefficients of the samples

	CH	SA	SE	PO	BA	NE	KA	Total
CH	14.1	12.7	11.3	5.6	16.9	33.8	5.6	100
SA	18.8	12.5	4.2	8.3	25.0	25.0	6.3	100
SE	12.7	3.6	58.2	5.5	5.5	5.5	9.1	100
PO	12.5	10.0	42.5	5.0	12.5	12.5	5.0	100
BA	5.8	21.2	13.5	11.5	21.2	19.2	7.7	100
NE	20.0	28.6	5.7	2.9	4.3	34.3	4.3	100
KA	0.0	8.7	6.5	0.0	13.0	0.0	71.7	100

Overall classification (cross-validated): 30.9%. The numbers in rows are percentages that denote the classification to the sampling sites given in columns (correctly classified samples are in bold)

Table 7 Dissimilarity matrix (below the diagonal) of average Euclidean distances based on otolith shape (CAP1, CAP2)

	CH	SA	SE	PO	BA	NE	KA
CH		114.92	142.75	187.98	390.2	435.4	553.08
SA	0.186		37.04	89.73	304.66	357.58	488.45
SE	2.525	3.704		52.69	267.64	320.82	452.62
PO	0.593	1.164	0.716		214.99	268.71	402.08
BA	0.242	0.190	2.511	0.570		60.64	202.04
NE	0.155	0.089	3.930	1.339	0.450		141.41
KA	4.339	3.524	5.738	3.789	2.530	4.727	

The geographic distances (in km) are presented above the diagonal

samples are distributed along a west-east axis in the SCB, we expected that geographic distance might play a major role in genetic and otolith shape affinities; however, these expectations were not entirely met.

Genetic studies have shown that freshwater teleosts often show significantly more population structure than do marine and anadromous species (e.g., McDowall 2001; Mehraban et al. 2020; Ward et al. 1994). In the SCB, the euryhaline fish, *P. gorlap* inhabits a wide diversity of sites encompassing the sea, inshore habitats, estuaries, rivers, wetlands and stream sources (Vasil'eva and Vasil'ev 2003; Zarei et al. 2021). It is similar to anadromous species with regard to its migratory behavior and capacity to move between brackish and freshwater environments. We thus found little population structure for *P. gorlap* in the SCB. Reproductive biology studies of *P. gorlap* from the northern and central sub-basins of the Caspian Sea basin described that it spawns on rocky and shingle bottoms (Ragimov 1968) in spring (April and May) when it moves inshore into shallow stony areas and rivers. It subsequently returns to deeper waters (6–12 m) in winter (Gaibova 1952; Ragimov 1968). The widespread distribution of the H1 haplotype in the SCB environments indicates high dispersal of *P. gorlap* throughout the Caspian Sea basin.

A preliminary phylogeographic analysis of 25 *P. gorlap* individuals using mitochondrial COI barcode sequences from 17 localities (15 in the SCB including 12 riverine and 3 inshore sites) in a broader phylogenetic context on Ponto-Caspian gobiids by Zarei et al. (2021) detected 33 variable nucleotide sites, which defined a total of 19 haplotypes, indicating high overall mtDNA variability of the species in the SCB ($Hd = 0.977$; $\pi = 0.009$; $k = 6.02$). Of these 19 haplotypes, two were shared between two localities, while the remainder were site-specific. Here, despite using the control region (vs. COI) for 90 individuals (vs. 25 individuals) from seven south Caspian localities (vs. 15 localities), its variability was low, and two of its 10 control region haplotypes were shared (H1 and H3) whereas the rest were site-specific. It should be noted that both are the same locus, since mtDNA is inherited as a single locus; thus, the two can be analyzed together. Based on both mtDNA

regions, the overall haplotype diversity of *P. gorlap* in the SCB is relatively high, however that per locality is generally low since most haplotypes are site-specific. This suggests that in addition to some migratory or mobile individuals, *P. gorlap* sites also contain resident individuals and samples (notably at KA).

All *P. gorlap* individuals from KA (the easternmost locality above the Zarrin Gol/Kaboudval Dam; Fig. 1) had haplotype H10, which was private to that sample. Φ_{ST} values between KA and the other samples were high, ranging from 0.77 to 1.00 ($P < 0.001$), as was its otolith shape differentiation. Restricted gene flow and isolated evolutionary histories under IBD or a refugial population scenario are expected to reveal a deep phylogeographic break between haplotypes, however, H10 and H1 differ by just a single mutational step. Additional studies using microsatellites or other nuclear DNA markers are warranted.

In comparison, the deepwater goby *Neogobius bathybius* (Kessler 1877), another endemic Caspian goby was found to have high gene flow across the southern Caspian Sea based on mtDNA COI and nuclear DNA S7 sequences (Tajbakhsh et al. 2022). As in the present results for *P. gorlap*, there were many haplotypes of *N. bathybius*, however, there were few significant differences among sampling sites; moreover, the species likely underwent significant population expansion about 247,000 years ago during the Pleistocene (Tajbakhsh et al. 2022), which differed from the present conclusions.

Otolith outline analysis using wavelet transformation revealed significant differences of *P. gorlap* samples that were positively correlated with genetic distances rather than with geographic distances among samples. The most distinct sample in terms of otolith morphology was also KA, which was much more prominent compared to its mitochondrial DNA differentiation (i.e., having a site-specific haplotype, H10, differing from H1 by one mutational step). This result can be explained by the fact that the morphological attributes apart from phylogenetic/population genetic factors may be influenced by environmental effects (Charmantier et al. 2005; Klingenberg 2010). Other studies have concluded that otolith shape is genetically determined, often species

specific, and may reflect phylogenetic and phylogeographic relationships (e.g., Reichenbacher et al. 2009; Zhuang et al. 2015). However, this may not necessarily reflect genetic differences. Otoliths show variations among conspecific individuals and many confounding effects have been suggested, such as different local environmental conditions or factors such as food availability, depth, water temperature, salinity, substrate type, and exposure to environmental contaminants (e.g., Cardinale et al. 2004; Schulz-Mirbach et al. 2008; Clark et al. 2021; Bidaye et al. 2022). In addition, among our *P. gorlap* samples, KA was the only one located in the Turan Plain freshwater ecoregion (other samples were in the Kura-South Caspian ecoregion; see Abell et al. 2008), which is the most arid part of the Transcaspian area. Rivers of the Turan Plain ecoregion, unlike the Kura-South Caspian ecoregion, are characterized by the features of rivers formed in arid regions, such as low flow, predominantly turbid and shallow, uneven regime, and considerable fluctuations in flow during the off-season. Regarding the morphological differentiation of the KA sample (see also Asgardoun et al. 2021), and since otolith morphology is known to evolve on ecological timescales and can signal the presence of cryptic lineages and species (Bidaye et al. 2022), additional sampling at KA and a nuclear DNA analysis could exclude a possible introgressive hybridization scenario.

Acknowledgements This study was supported by Shiraz University (SU-9630190). We thank Y. Bakhshi for fieldwork help. We are very grateful to Carol A. Stepien (National Museum of Natural History, USA), who has improved and corrected this work by her gobiological knowledge and with her editing skills.

Data availability The DNA sequences and specimens are available in GenBank (ON724062–ON724151) and ZM-CBSU, respectively.

Declarations

Conflict of interest The authors declare no conflict of interest.

Ethical approval This study was approved by the Ethics Committee of the Biology Department of Shiraz University.

References

- Abell R, Thieme ML, Revenga C, Bryer M, Kottelat M, Bogutskaya N, Coad B, Mandrak N, Balderas SC, Bussing W, Stiassny ML (2008) Freshwater ecoregions of the world: a new map of biogeographic units for freshwater biodiversity conservation. *Bioscience* 58:403–414
- Asgardoun S, Patimar R, Golzarianpour K, Eagderi S (2021) Geometric morphology of Iranian goby *Ponticola iranicus* Vasil'eva, Mousavi-Sabet & Vasil'ev, 2015 in the Southern Caspian Sea basin. *Taxon Biosyst* 13:19–32 (in Persian)
- Avise JC, Arnold J, Ball RM, Bermingham E, Lamb T, Neigel JE, Reeb CA, Saunders NC (1987) Intraspecific phylogeography: the mitochondrial DNA bridge between population genetics and systematics. *Annu Rev Ecol Evol Syst* 18:489–522
- Berg LS (1949) Freshwater fishes of the USSR and adjacent countries. Israel Program for Scientific Translations, Jerusalem
- Berg F, Almeland OW, Skadal J, Slotte A, Andersson L, Folkvord A (2018) Genetic factors have a major effect on growth, number of vertebrae and otolith shape in Atlantic herring (*Clupea harengus*). *PLoS One* 13:e0190995
- Bidaye RG, Al-Jufaili SM, Charmpila EA, Jawad L, Vukić J, Reichenbacher B (2022) Possible links between phenotypic variability, habitats and connectivity in the killifish *Aphaniops stoliczkanus* in Northeast Oman. *Acta Zool.* <https://doi.org/10.1111/azo.12428>
- Boldyrev VS, Bogutskaya NG (2007) Revision of the tadpole-gobies of the genus *Benthophilus* (Teleostei: Gobiidae). *Ichthyol Explor Freshw* 18:31–96
- Brown JE, Stepien CA (2008) Ancient divisions, recent expansions: phylogeography and population genetics of the round goby *Apollonia melanostoma*. *Mol Ecol* 17:2598–2615
- Bruford MW, Hanotte O, Brookfield JF, Burke T (1992) Single-locus and multilocus DNA fingerprinting. In: Hoezel C (ed) *Molecular genetics analysis of populations: a practical approach*. Oxford University Press, NY, pp 225–269
- Cardinale M, Doering-Arjes P, Kastowsky M, Mosegaard H (2004) Effects of sex, stock, and environment on the shape of known-age Atlantic cod (*Gadus morhua*) otoliths. *Can J Fish Aquat Sci* 61:158–167
- Charmantier A, Garant D (2005) Environmental quality and evolutionary potential: lessons from wild populations. *Proc R Soc B: Biol Sci* 272:1415–1425
- Clark FJK, da Silva Lima CS, Pessanha ALM (2021) Otolith shape analysis of the Brazilian silverside in two northeastern Brazilian estuaries with distinct salinity ranges. *Fish Res* 243:106094
- Crookes S, Shaw PW (2016) Isolation by distance and non-identical patterns of gene flow within two river populations of the freshwater fish *Rutilus rutilus* (L. 1758). *Conserv Genet* 17:861–874
- Dixon P (2003) VEGAN, a package of R functions for community ecology. *J Veg Sci* 14:927–930
- Eagderi S, Nikmehr N, Poorbagher H (2020) *Ponticola patimari* sp. nov. (Gobiiformes: Gobiidae) from the southern Caspian Sea basin. *Iran FishTaxa* 17:22–31
- Esmaeili HR, Coad BW, Mehraban HR, Masoudi M, Khaefi R, Abbasi K, Mostafavi H, Vatandoust S (2015) An updated checklist of fishes of the Caspian Sea basin of Iran with a note on their zoogeography. *Iran J Ichthyol* 1:152–184
- Esmaeili HR, Sayyadzadeh G, Zarei F, Kafaei S, Coad BW (2020) Phylogeographic pattern and population structure of the Persian stone loach, *Oxynoemacheilus persa* (Heckel 1847) (family: Nemacheilidae) in southern Iran with implications for conservation. *Environ Biol Fishes* 103:77–88
- Excoffier L, Lischer HE (2010) Arlequin suite ver 3.5: a new series of programs to perform population genetics analyses under Linux and Windows. *Mol Ecol Resour* 10:564–567
- Forte AM, Cowgill E (2013) Late Cenozoic base-level variations of the Caspian Sea: a review of its history and proposed driving mechanisms. *Palaeogeogr Palaeoclimatol Palaeoecol* 386:392–407
- Gaibova RA (1952) Gobies from the Schihovo-Karadagskii region of the Caspian Sea. *Proc Zool Inst Acad Sci SSSR* 15:53–106 (in Russian)
- Gante HF, Micael J, Oliva-Paterna FJ, Doadrio I, Dowling TE, Alves MJ (2009) Diversification within glacial refugia: tempo and mode of evolution of the polytypic fish *Barbus sclateri*. *Mol Ecol* 18:3240–3255
- Gierl C, Liebl D, Sanda R, Vukic J, Esmaeili HR, Reichenbacher B (2018) What can goby otolith morphology tell us? *Cybium* 42:349–363
- Gill AC, Mooi RD (2012) Thalasseleotrididae, new family of marine gobioid fishes from New Zealand and temperate Australia, with

- a revised definition of its sister taxon, the Gobiidae (Teleostei: Acanthomorpha). *Zootaxa* 3266:41–52
- Günther A (1861) Catalogue of the fishes in the British Museum. Catalogue of the Acanthopterygian fishes in the collection of the British Museum. Gobiidae, Discoboli, Pediculati, Blenniidae, Labyrinthici, Mugilidae, Notacanthi. Taylor and Francis, London
- Hall TA (1999) BioEdit: a user-friendly biological sequence alignment editor and analysis program for Windows 95/98/NT. *Nucleic Acids Symp Ser* 41:95–98
- Hammer Ø, Harper DA, Ryan PD (2001) Paleontological statistics software package for education and data analysis. *Palaeontol Electron* 4:1–9
- Ihaka R, Gentleman R (1996) R: a language for data analysis and graphics. *J Comput Graph Stat* 5:299–314
- Ilijn BS (1927) Keys to the gobies (Fam. Gobiidae) of the sea of Azov and the black sea preliminary communication. *Trudy Azovsko-Cernomorskoi Naučno-Promyslovoj Ėkspedicii* 2:128–143 (in Russian)
- Ilijn BS (1956) Remarks and corrections to suborder Gobioidi in the book of L. S. Berg "Freshwater fishes of the USSR and neighboring countries", edit. 4, 1948–1949. *Vopr Ikhtyologii* 7:1055–1125 (in Russian)
- Kessler KF (1874) A description of fishes belonging to the families' common to both the Black and the Caspian seas. *Trudy St Petersburg Obsc Estestvoisp* 5:191–324 (in Russian)
- Kessler KF (1877) The Aralo-Caspian expedition. IV. Pontine ichthyological region. *Naturgeschichte der Fische Islands, St. Petersburg*
- Kimura M (1983) The neutral theory of molecular evolution. Cambridge University Press, Cambridge
- Klingenberg CP (2010) Evolution and development of shape: integrating quantitative approaches. *Nat Rev Genet* 11:623–635
- Krijgsman W, Tesakov A, Yanina T, Lazarev S, Danukalova G, Van Baak CG, Agustí J, Alçiçek MC, Aliyeva E, Bista D, Bruch A (2019) Quaternary time scales for the Pontocaspian domain: interbasinal connectivity and faunal evolution. *Earth Sci Rev* 188:1–40
- Kumar S, Stecher G, Tamura K (2016) MEGA7: molecular evolutionary genetics analysis version 7.0 for bigger datasets. *Mol Biol Evol* 33:1870–1874
- Leigh JW, Bryant D (2015) POPART: full-feature software for haplotype network construction. *Methods Ecol Evol* 6:1110–1116
- Librado P, Rozas J (2009) DnaSP v5: a software for comprehensive analysis of DNA polymorphism data. *Bioinformatics* 25:1451–1452
- Libungan LA, Pálsson S (2015) ShapeR: an R package to study otolith shape variation among fish populations. *PLoS One* 10:e0121102
- Libungan LA, Óskarsson GJ, Slotte A, Jacobsen JA, Pálsson S (2015) Otolith shape: a population marker for Atlantic herring *Clupea harengus*. *J Fish Biol* 86:1377–1395
- McDowall RM (2001) Diadromy, diversity and divergence: implications for speciation processes in fishes. *Fish Fish* 2:278–285
- Mehraban H, Esmaili HR, Zarei F, Ebrahimi M, Gholamhosseini A (2020) Genetic diversification, population structure, and geophylogeny of the Scarface rockskipper *Istiblennius pox* (Teleostei: Blenniidae) in the Persian Gulf and Oman Sea. *Mar Biodivers* 50:1–12
- Miller PJ (2003) The freshwater fishes of Europe, Vol. 8/I Mugilidae, Atherinidae, Atherinopsidae, Blenniidae, Odontobutidae, Gobiidae 1. AULA-Verlag GmbH Wiebelsheim, Verlag für Wissenschaft und Forschung, Germany
- Miller PJ (2004) The freshwater fishes of Europe Vol. 8/II Gobiidae 2. AULA-Verlag GmbH Wiebelsheim, Verlag für Wissenschaft und Forschung, Germany
- Mousavi-Sabet H (2021) Dams and their impacts on fishes in Iran. In: Jawad LA (ed), Tigris and Euphrates rivers: their environment from headwaters to mouth. *Aquatic Ecology Series*, Vol 11. Springer, Cham, pp 401–420
- Naseka NM, Bogutskaya NG (2009) Fishes of the Caspian Sea: zoogeography and updated check-list. *Zoosyst Ross* 18:295–317
- Nason G (2016) Package 'wavethresh': wavelets statistics and transforms. CRAN
- Neilson ME, Stepien CA (2009) Escape from the Ponto-Caspian: evolution and biogeography of an endemic goby species flock (Benthophilinae: Gobiidae: Teleostei). *Mol Phylogenet Evol* 52:84–102
- O'Dwyer JE, Murphy N, Tonkin Z, Lyon J, Koster W, Dawson D, Amtstaetter F, Harrison KA (2021) An investigation of genetic connectivity shines a light on the relative roles of isolation by distance and oceanic currents in three diadromous fish species. *Mar Freshw Res* 72:1457–1473
- Oksanen J, Blanchet FG, Friendly M, Kindt R, Legendre P, McGlinn D (2020) Package 'vegan': community ecology package. CRAN
- Ostellari L, Bargelloni L, Penzo E, Patarnello P, Patarnello T (1996) Optimization of single-strand conformation polymorphism and sequence analysis of the mitochondrial control region in *Pagellus bogaraveo* (Sparidae, Teleostei): rationalized tools in fish population biology. *Anim Genet* 27:423–427
- Ouborg NJ, Pertoldi C, Loeschcke V, Bijlsma RK, Hedrick PW (2010) Conservation genetics in transition to conservation genomics. *Trends Genet* 26:177–187
- Peters A, Hothorn T, Ripley BD, Therneau T, Atkinson B (2021) Package 'ipred': improved predictors. CRAN
- Ragimov DB (1968) The distribution of gobies of west coasts of the Middle and South Caspian. *Izv Akad Nauk Azerbaidzhansk SSR Ser Biol* 4:66–74 (in Russian)
- Reichenbacher B, Bannikov AF (2022) Diversity of gobioid fishes in the late middle Miocene of northern Moldova, Eastern Paratethys—part I: an extinct clade of *Lesueurigobius* look-alikes. *PalZ* 96:67–112
- Reichenbacher B, Feulner GR, Schulz-Mirbach T (2009) Geographic variation in otolith morphology among freshwater populations of *Aphanius dispar* (Teleostei, Cyprinodontiformes) from the southeastern Arabian Peninsula. *J Morphol* 270:469–484
- Reichenbacher B, Sienknecht U, Küchenhoff H, Fenske N (2007) Combined otolith morphology and morphometry for assessing taxonomy and diversity in fossil and extant killifish (*Aphanius*, †*Prolebias*). *J Morphol* 268:898–915
- Reid DF, Orlova MI (2002) Geological and evolutionary underpinnings for the success of Ponto-Caspian species invasions in the Baltic Sea and North American Great Lakes. *Can J Fish Aquat Sci* 59:1144–1158
- Ripley B, Venables B, Bates DM, Hornik K, Gebhardt A, Firth D (2021) Package 'MASS': functions and datasets to support Venables and Ripley. "Modern Applied Statistics with S". CRAN
- Sadeghi R, Esmaili HR, Zarei F, Reichenbacher B (2020) Population structure of the ornate goby, *Istigobius ornatus* (Teleostei: Gobiidae), in the Persian Gulf and Oman Sea as determined by otolith shape variation using ShapeR. *Environ Biol Fishes* 103:1217–1230
- Sands AF, Neubauer TA, Nasibi S, Harandi MF, Anistratenko VV, Wilke T, Albrecht C (2019) Old lake versus young taxa: a comparative phylogeographic perspective on the evolution of Caspian Sea gastropods (Neritidae: *Theodoxus*). *R Soc Open Sci* 6:190965
- Schulz-Mirbach T, Stransky C, Schlickeisen J, Reichenbacher B (2008) Differences in otolith morphologies between surface- and cave-dwelling populations of *Poecilia mexicana* (Teleostei, Poeciliidae) reflect adaptations to life in an extreme habitat. *Evol Ecol Res* 10:537–558

- Schwarzahns W, Brzobohaty R, Radwanska U (2020) Goby otoliths from the Badenian (Middle Miocene) of the Central Paratethys from the Czech Republic, Slovakia and Poland: a baseline for the evolution of the European Gobiidae (Gobiiformes; Teleostei). *Boll Soc Paleontol Ital* 59:125–173
- Slatkin M (1993) Isolation-by-distance in equilibrium and non-equilibrium populations. *Evolution* 47:264–279
- Stepien CA, Kocher TD (1997) Molecules and morphology in studies of fish evolution. In: Kocher TD, Stepien CA (eds) *Molecular Systematics of Fishes*. Academic Press, San Diego, pp 1–11
- Tajbakhsh F, Rajabi-Maham H, Abdoli A, Stepien CA, Kiabi BH (2022) DNA sequence support for re-classification of the endemic south Caspian Sea deepwater goby as *Neogobius bathybius* (from *Ponticola*; Perciformes: Gobiidae) and recent population expansion of a continuous population. *Ichthyol Herpetol* 110:13–21
- Vasil'ev VP, Vasil'eva ED (1992) Karyological evidence of the separate species status of *Neogobius kessleri* (Günther) and *Neogobius gorlap* Iljin (Pisces, Gobiidae). *Dokl Akad Nauk SSSR* 324:898–900 (in Russian)
- Vasil'eva ED, Vasil'ev VP (1996) The description of *Neogobius iljini* sp. nov. within former *N. kessleri* (Gobiidae, Pisces). *Acta Univ Carol Biol* 39:261–270
- Vasil'eva ED, Vasil'ev VP (2003) *Neogobius gorlap* Iljin in Berg, 1949. In: Miller PJ (ed) *The freshwater fishes of Europe*, Vol. 8/I Mugilidae, Atherinidae, Atherinopsidae, Blenniidae, Odontobutidae, Gobiidae 1. AULA-Verlag GmbH Wiebelsheim, Verlag für Wissenschaft und Forschung, Germany, pp 253–264
- Vasil'eva ED, Mousavi-Sabet H, Vasil'ev VP (2015) *Ponticola iranicus* sp. nov. (Actinopterygii: 1203 Perciformes: Gobiidae) from the Caspian Sea basin. *Acta Ichthyol Piscat* 45:189–197
- Vasil'eva ED, Schwarzahns WW, Medvedev DA, Vasil'ev VP (2016) Cryptic species of Ponto-Caspian bighead goby of the genus *Ponticola* (Gobiidae). *J Ichthyol* 56:1–18
- Vasil'eva ED, Vasil'ev VP (1996) The description of *Neogobius iljini* sp. nov. within former *N. kessleri* (Gobiidae, Pisces). *Acta Univ Carol Biol* 39:261–270
- Ward RD, Woodwark M, Skibinski DO (1994) A comparison of genetic diversity levels in marine, freshwater, and anadromous fishes. *J Fish Biol* 44:213–232
- Warnes G, Bolker B, Bonebakker L, Gentleman R, Huber W (2020) Package 'gplots': various R programming tools for plotting data. CRAN
- Zarei F, Esmaeili HR, Abbasi K, Kovačić M, Schliewen UK, Stepien CA (2022a) Gobies (Teleostei: Gobiidae) of the oldest and deepest Caspian Sea sub-basin: an evidence-based annotated checklist and a key for species identification. *Zootaxa* 5190:151–193
- Zarei F, Esmaeili HR, Sadeghi R, Schliewen UK, Kovačić M, Abbasi K, Gholamhosseini A (2022b) An integrative insight into the diversity, distribution, and biogeography of the freshwater endemic clade of the *Ponticola syrman* group (Teleostei: Gobiidae) in the Caucasus biodiversity hotspot. *Ecol Evol* 12:e9300
- Zarei F, Esmaeili HR, Schliewen UK, Abbasi K (2022c) Taxonomic diversity and distribution of the genus *Proterorhinus* (Teleostei: Gobiidae) in the Caucasus biodiversity hotspot with conservation implications. *Aquat Conserv: Mar Freshw Ecosyst* 32:129–138
- Zarei F, Esmaeili HR, Schliewen UK, Abbasi K, Sayyadzadeh G (2021) Mitochondrial phylogeny, diversity, and ichthyogeography of gobies (Teleostei: Gobiidae) from the oldest and deepest Caspian sub-basin and tracing source and spread pattern of an introduced *Rhinogobius* species at the tricontinental crossroad. *Hydrobiologia* 848:1267–1293
- Zhuang L, Ye Z, Zhang C (2015) Application of otolith shape analysis to species separation in *Sebastes* spp. from the Bohai Sea and the Yellow Sea, northwest Pacific. *Environ Biol Fishes* 98:547–558

Publisher's Note Springer Nature remains neutral with regard to jurisdictional claims in published maps and institutional affiliations.

Springer Nature or its licensor (e.g. a society or other partner) holds exclusive rights to this article under a publishing agreement with the author(s) or other rightsholder(s); author self-archiving of the accepted manuscript version of this article is solely governed by the terms of such publishing agreement and applicable law.